JACS
JOURNAL OF THE AMERICAN CHEMICAL SOCIETY

Article

pubs.acs.org/JACS

Stereochemistry-Dependent, Mechanoresponsive Supramolecular Host Assemblies for Fullerenes: A Guest-Induced Enhancement of Thixotropy

Arnab Dawn,[†] Tomohiro Shiraki,[‡] Hiroshi Ichikawa,[§] Akihiko Takada,[§] Yoshiaki Takahashi,[§] Youichi Tsuchiya,[‡] Le Thi Ngoc Lien,[∥] and Seiji Shinkai*[,†,‡]

[†]Institute for Advanced Study and [∥]Department of Applied Chemistry, Faculty of Engineering, Kyushu University, 744 Moto-oka, Nishi-ku, Fukuoka 819-0395, Japan

[‡]Nanotechnology Laboratory, Institute of Systems, Information Technologies and Nanotechnologies, 203-1 Moto-oka, Nishi-ku, Fukuoka 819-0385, Japan

[§]Evaluation Office of Materials Properties and Function and Department of Advanced Device Materials, Institute for Materials Chemistry and Engineering, Kyushu University, 6-1 Kasuga-koen, Kasuga-city, Fukuoka 816-8580, Japan

Supporting Information

ABSTRACT: Self-assembly behaviors of a series of systems (**G1**, **G2**, and **G3**) possessing same organic building blocks based on a substituted anthracene have been investigated in decalin. **G2** and **G3** are dominated by head-to-tail (ht) and head-to-head (hh) type dimers of **G1**, respectively. **G1** gives a thermoresponsive gel that behaves ideally, showing frequency-independent elastic and viscous moduli. Interestingly, **G2** produces a thixotropic gel that shows the signature of structural relaxation, signifying the dynamic nature of the system. In contrast, **G3** remains fluidlike. As investigated by scanning electron microscopy (SEM), in the assembly process of **G2**, first disklike nanoaggregates are formed, and in the second step these aggregates interact to construct the densely packed secondary assembly. A transition from secondary assembly to primary assembly under shear initiates the mechanoresponsive destruction of the gel. In the self-assembly process, **G1** propagates in a one-dimensional fashion, whereas **G2** and **G3** can propagate in a two-dimensionional fashion. The same side orientation of the substituents in **G3** facilitates the formation of a compact closed-shell-type structure, which results in the generation of isolated nanocrystals. The long-range weak interaction together with the capability of propagating in two dimensions is found to be essential for the construction of such a mechanoresponsive assembly. C_{60} and C_{70} could be incorporated successfully in **G2** assembly to develop mechanoresponsive fullerene assemblies. The presence of fullerenes not only enhances the elastic properties of **G2** but also intensifies the thixotropy. C_{70} appears to be a superior guest in terms of property enhancement due to its better size fitting with the concave-shaped host.

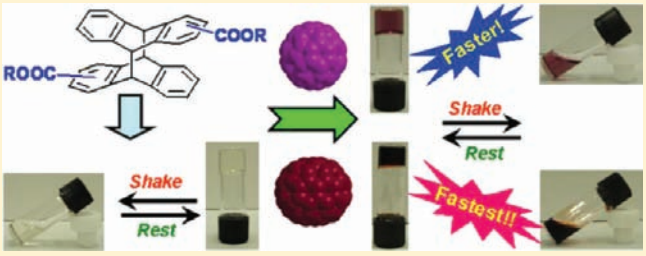

INTRODUCTION

Stimuli-responsive supramolecular assemblies represent a smart class of materials that exhibit dramatic changes in their molecular organization in response to the external stimuli such as temperature, light, pH, chemicals, electricity, mechanical stress, etc. The beauty of the supramolecular chemistry lies in its unique reversibility between the integrated and disintegrated phases driven by the collective contributions from different kinds of noncovalent interactions including hydrogen bonding, $\pi-\pi$ stacking, van der Waals, metal−ligand interactions, etc.[1] Organogels[2] are an important subclass in this field and can be tailored to respond against different stimuli.[2h,3] However, developing programmable supramolecular gel materials still remains a matter of challenge.[4] From a chemistry viewpoint, it appears to be feasible to develop photo-, chemo-, or redox-responsive assemblies by introducing photoactive, chemically active, or redox-active functional groups, respectively, into the building blocks.[2h] However, a mechanoresponsive functional group is still an undisclosed entity. On the positive side of the frame, there are a few reports on the mechanical activation of the covalent bonds,[5] which frequently involves the use of so-called mechanophores or noncovalent mechanochemistry composed of biological systems.[6] In those cases, the mechanical trigger enables changes to the molecules individually or locally. However, stimulating a molecular ensemble mechanically, maintaining the reversibility, and especially the design of such a system still remains a matter of serendipity. Therefore, it is not surprising that the reports on small molecular thixotropic materials are rather limited.[7] Revealing a believable mechanism correlating the molecular building blocks with the macroscopic output would perhaps

Received: September 16, 2011
Published: December 28, 2011

   dx.doi.org/10.1021/ja211032m | J. Am. Chem.Soc. 2012, 134, 2161−2171

Scheme 1. Formation of Dimeric Systems G2 and G3 from Monomeric Gelator G1 by Photodimerization and Structures of Fullerenes Used As Guest Molecules

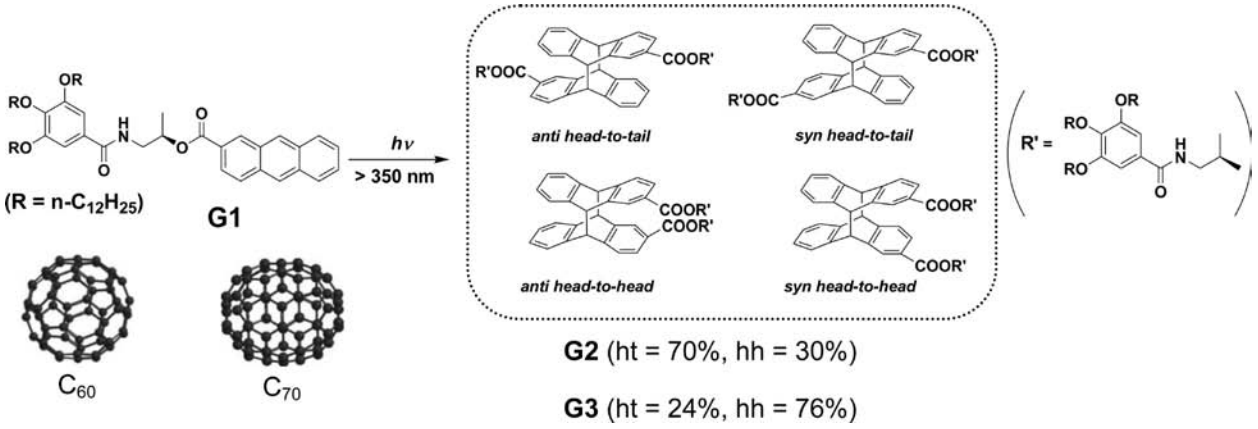

Table 1. Gelation Behavior and Responsiveness of Samples Prepared from G1 and G2 in Different Organic Solvents[a]

	G1		G2	
solvent	observation (quenching temp, °C)	responsiveness	observation (quenching temp, °C)	responsiveness
n-hexane	gel (20)	thermal only	gel (20)	thixotropic
cyclohexane	weak gel (10)	thermal only	weak gel (20)	not distinct
methylcyclohexane	gel (5)	thermal only	gel (20)	thixotropic
decalin (cis/trans)	gel (5)	thermal only	gel (20)	thixotropic

[a]The gelator concentration in each case was maintained at 2% (w/v).

improve this situation. To take this challenge, herein, we developed a mechanoresponsive host assembly system (**G2**) composed of dianthracene units prepared from the parent anthracene-based gelator (**G1**) showing only thermoresponsiveness. Moving a step forward to the next stage, such a unique host assembly is utilized to immobilize and mobilize fullerene molecules reversibly under mechanical stimuli. Extracting the essence of these studies, here we propose, for the first time, a clear structure–function correlation behind the construction of a mechanoresponsive assembly.

Recently, we succeeded in performing supramolecular photochirogenesis in gel media using a series of organogelators having a 2-substituted anthracenecarboxylic acid moiety (Scheme 1).[8] During the course of this investigation, we had noticed that while the gel systems dominated by head-to-head (hh) gelator orientation underwent photoinduced gel-to-sol phase transition, the systems dominated by head-to-tail (ht) gelator orientation experienced an increase in their gel melting temperatures as the result of photodimerization. The second point of interest was the structural and chemical modification of the planar (or nearly planar) anthracene, which changes to a bent dianthracene having isolated benzene rings. This would modify and "soften" the intermolecular interactions significantly, and the system is expected to offer some dynamic phenomenon that may facilitate a response against mechanical stimuli. As per our prediction, indeed the photodimers dominated by the ht orientation form a thixotropic gel, whereas the system composed of mostly hh photodimers appears as fluid.

The importance of such a stimuli-responsive assembly can be enhanced even further if it becomes capable of incorporating and releasing the functional guest molecules reversibly under stimuli. There are a few reports where molecular receptors for fullerenes were designed on the basis of concave–convex complementarity.[9] In those cases, the large surface to volume ratio of fullerenes facilitates van der Waals interaction, which plays the most prominent role in complex formation. We envisioned that the self-assembled dianthracene-based gelator might promote such a binding mode, with additional supramolecular interactions available for the gelator organization, and at the same time the incorporated fullerenes might act like a molecular adhesive, influencing the dynamic nature of the assembly. Very interestingly, **G2** assembly could incorporate both C_{60} and C_{70}. It is worth noting that, in the presence of added fullerenes, the thixotropic behavior of the assembly becomes pronounced and C_{70} demonstrates superior interaction and responsiveness. To the best of our knowledge, this is the first report of a fullerene-bearing mechanoresponsive assembly.

In the present study, the mechanoresponsive behavior of **G2** assembly in the presence and the absence of fullerenes has been investigated with the help of rheological experiments. The growth and destruction processes of such an assembly are closely studied for the first time, with the aid of scanning electron microscopy (SEM). The thermoresponsive **G1** gel is investigated simultaneously to draw a correlation and also to differentiate between two systems. Binding of fullerenes to the gelator assembly is estimated and discussed in a qualitative manner. Finally, we have made a genuine attempt to shed light on the mechanistic ground behind the growth of a mechanoresponsive assembly with the help of molecular modeling and illustrations based on the experimental results.

RESULTS AND DISCUSSION

Sample Preparation and Self-Assembling Behaviors. Dimeric systems have been prepared by the stereoselective photodimerization of monomeric gelator **G1** under specific solvent and reaction conditions (Scheme 1). In the present study, two types of dimer mixtures have been investigated,

dx.doi.org/10.1021/ja211032m | J. Am. Chem.Soc. 2012, 134, 2161–2171

namely, **G2** and **G3**. They differ in the relative proportions of hh and ht dimers. While **G2** prepared in tetrahydrofuran (THF) at 40 °C involves 70% ht dimers, **G3** prepared in methylcyclohexane at 30 °C consists of 76% hh dimers (Supporting Information, Table S1). In both cases the monomer to dimer conversion was almost exclusive (more than 90%) as confirmed from UV−vis and NMR spectra (Supporting Information, Figures S1 and S2).

We have tested the gelation behaviors of **G2** and **G3** in organic solvents by dissolving the solid samples at high temperature (50−60 °C) and then quenching at 20 °C. Interestingly, while **G3** remained fluid in all solvents tested here, **G2** underwent gelation in a series of nonpolar solvents like *n*-hexane, methylcyclohexane, and decalin, similar to what we observed earlier for **G1** (Table 1).[8c] Moreover, in contrast to **G1** gels, which show only thermoresponsiveness, the gels prepared from **G2** become fluid under shaking and recover to the gel state upon resting (Supporting Information, Figure S3). This is a unique phenomenon called thixotropy. We can repeat this reversible phase transition many times without affecting the overall appearance or the stability. These materials are also stable for months without any phase separation. As expected, **G2** gels can also be disintegrated and integrated reversibly by heating and quenching at room temperature, respectively. The recovery time of the gel after destruction by thermal stimulation is much longer (10−12 h) than it is after mechanical stimulation [about 1 h for a 1.8% (w/v) gel in decalin]. It is worth mentioning here that **G2** gels can also be prepared by mixing the gelator and the solvent at room temperature (20 °C) and they still show mechanoresponsiveness. However, to avoid any artifact arising from inhomogeneity, we have carried out all the experiments with samples homogenized by heating only. Also, considering the higher boiling point and viscosity (good for rheological measurements), we have chosen decalin as the gelating solvent to prepare the samples for different experiments. Thus, unless otherwise mentioned, decalin was the solvent used to prepare the samples. Another striking feature of **G2** gels is that the gelation occurs only near room temperature. Quenching the homogenized solution of **G2** at −20 to 5 °C did not result in any gel formation even after a week. However, when we kept the same mixture at 20 °C, it turned into a gel within an hour. This signifies the indispensability of thermal motion in construction of the gel structure. We shall highlight this point later.

Behaviors of Self-Assembled Systems under Mechanical Stimuli, Studied by Rheology. The reversible phase transition of an assembly under mechanical stimuli can be followed best by rheological measurements. In our study, we have monitored the storage modulus G', associated with energy storage, and the loss modulus G'', associated with dissipation of energy, of different assembled systems as functions of shear stress, angular frequency, and time. We were interested to test, first, whether the current system represents a "true gel", and second, whether our system is indeed dynamic. To reveal these, the frequency dependency of **G2** gel has been studied by dynamic frequency sweep experiment (Figure 1). Very interestingly, the elastic and viscous moduli show frequency dependency. In the higher-frequency region (ω > 19.8 rad/s) the sample behaves like a gel ($G' > G''$), whereas in the low-frequency region (ω < 19.8 rad/s), the sample shows fluidlike behavior ($G'' > G'$). This means, therefore, that at low frequencies the assembly carries the signature of a structural relaxation process[10] where the viscous modulus approaches the

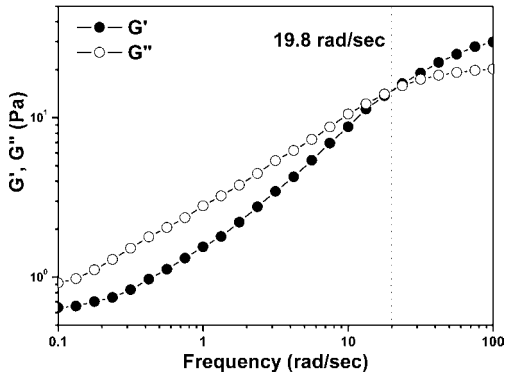

Figure 1. Frequency dependence of storage modulus G' and loss modulus G'' of **G2** assembly in decalin (1.8% w/v) performed at 20 °C under a constant 1% strain.

elastic modulus with decreasing frequency, and after the crossing over ($G'' > G'$) it decreases along with G'. This behavior more resembles the wormlike micelles that are known to entangle at high concentration, giving rise to a characteristic viscoelastic behavior similar to that found in transient polymer networks.[11] It signifies that when a deformation is applied, the assembled phase will revert back to the equilibrium after some time. Now, if the applied shear has a shorter time period compared to the relaxation time of the system, it behaves like an elastic gel. On the other hand, if the arrangement is deformed slowly, it behaves like a viscous fluid. This finding strongly supports the dynamic nature of **G2** gel. Since the present system does not satisfy the criteria for a "true gel", henceforth, **G2** gel should be considered as a "gel-like" material. Also, to carry out the viscoelastic measurements in the assembled state, we shall perform all the rheological experiments at a higher angular frequency domain where the sample behaves more or less like a gel.

The next step of the experiment consists of determining the so-called linear regime of **G2** gel. This was done by measuring G' and G'' as a function of applied stress (Supporting Information, Figure S4). From this experiment, we determined the yield stress value (i.e., stress at which G' deviates from linearity) as 1.61 Pa for the system. Another striking feature is that the assembly appeared to be broken into a two-step process, which is rather unusual in a rheological measurement. Probably this feature is associated with the multiple growth process of the assembly. A detailed discussion will be done later. A small increase in G'' value near this region probably indicates the local rearrangement in the sample.[12]

To study the most promising property of the sample, that is, the thixotropic behavior, **G2** gel was sheared at a constant shear stress of 10 Pa for 1 min. At the beginning of the experiment, the mechanical stress was released and the gel recovery was monitored by measuring the time evolution of G' and G'' (Figure 2). Here, a low strain (1%) was applied in order to avoid a perturbation of the assembly. At the initial stage of the recovery experiment, when the sample is destroyed mechanically, it is more viscous than elastic ($G'' > G'$). However, with time the sample recovers its elastic property and behaves as a gel-like material ($G' > G''$). The storage modulus G' increased and leveled to a value of 28 Pa. This experiment can be repeated many times (we have repeated three times) on the same gel and each time the gel recovers its elastic properties without being heated and cooled. Clearly, **G2** assembly demonstrates the mechanoresponsive behavior, where it breaks

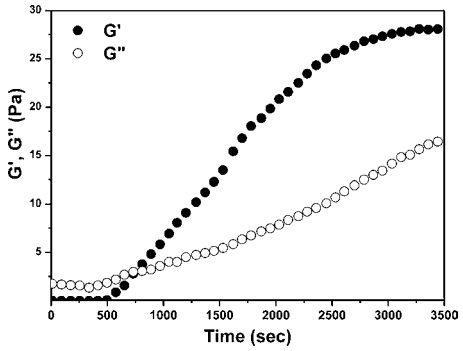

Figure 2. Evolution of storage modulus G' and loss modulus G'' as a function of time for **G2** assembly in decalin (1.8% w/v) performed at 20 °C under 1% strain and at a frequency 100 rad/s.

under shear and heals once the stress is released. As expected, **G3** does not show any significant reversible changes in the values of G' or G'' (which were too small to detect accurately) under the application or release of the applied shear (Supporting Information, Figure S5). Thus, it is clear that the stereochemistry of the gelator plays the crucial role in forming the gel-like assembly and also in demonstrating thixotropic behavior.[13] So far, such a scenario has not been addressed well for low molecular weight gelators (LMGs).

Previously, we examined the gelation properties of **G1**;[8c] however, a rheological study was not performed. Here it has become indispensable for us to examine and compare a thermoresponsive assembly (arising from **G1**) with a chemically similar but mechanoresponsive assembly prepared from **G2**. Since **G1** can form the gel at low temperature only, first we introduced the hot homogeneous solution of **G1** in the rheometer plate maintained at 5 °C, and gel formation was monitored by measuring G' and G'' as a function of time (Supporting Information, Figure S7). After about 1 h, the storage modulus reached a maximum and leveled at 909 Pa, which is more than 30-fold higher than that of **G2** gel recovered after the release of mechanical stress. In the frequency sweep experiment, **G1** gel behaved rather ideally where the storage and loss moduli were practically independent of frequency (Supporting Information, Figure S8). The yield stress value determined from the stress sweep experiment was found to be 38.8 Pa (Supporting Information, Figure S9), which is again more than 20-fold higher than that of **G2**. It is very clear from these findings that **G1** assembly is mechanically robust compared to **G2** assembly. To confirm about the responsiveness, we have performed a recovery experiment with **G1** gel after its shear-induced destruction. As expected, even after a few hours there was no significant recovery of the storage modulus (Supporting Information, Figure S10). Unlike **G2**, therefore, **G1** assembly is not mechanoresponsive but shows only thermoresponsiveness.

Thus, from the above rheological studies, one can clearly distinguish between a thermoresponsive and a mechanoresponsive supramolecular assembly constructed by **G1** and **G2**, respectively.

Morphological Studies on the Self-Assembled Systems. Electron microscopy provides a visual image of the aggregation behavior of a self-assembled system. Especially, direct visualization of a mechanoresponsive assembled system on the nanometer scale is very rare;[7h] visualization is mostly limited to optical microscopy for the detection of crystalline superstructures or for large fibrous aggregates having dimensions of several micrometers.[7c,e,14] Using our systems here, for the first time, we could observe such a mechanoresponsive assembly closely with the help of SEM under different situations. Figure 3 presents SEM images of **G2**

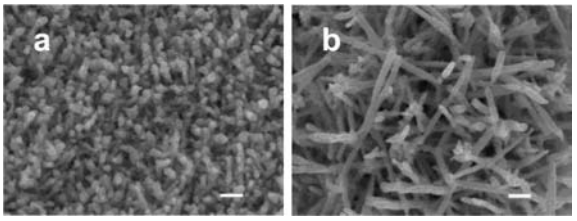

Figure 3. SEM micrographs of **G2** gels in decalin (1.5% w/v) prepared at 20 °C by homogenization at (a) 50 °C and (b) 20 °C (scale bar = 1 μm).

gels prepared from the mixture homogenized at 50 °C (Figure 3a) as well as at 20 °C (Figure 3b). While both images demonstrate the rodlike morphology, the latter has a smoother surface and higher aspect ratio. Interestingly, we captured the existence of mixed morphologies for the sample homogenized at room temperature (Supporting Information, Figure S11). Probably, this result is associated with the multiple nucleation processes arising from the inhomogeneity that may exist in the mixture.

We have followed the formation and breaking (by shear) of **G2** gel in decalin at 20 °C by SEM (Figure 4). At the initial stage (after 2 h in Figure 4a), the morphology consists of isolated disklike aggregates of irregular shapes with an average diameter of 300 nm. With the progress of time, the isolated aggregates gather to become more closely packed ones, facilitating the interaction among them (see Figure 4b after 5 h). Up to this stage, the appearance of the sample is still sol-like. After 10 h (Figure 4c), the isolated blocks are no longer visible; instead they form one-dimensional aggregates. At this stage, the sample starts to show gel-like behavior. Finally, after formation of a stable gel (Figure 4d, after 24 h), the one-dimensional structure becomes more prominent. It is worth noticing that after application of shear to the gel (sample collected from the rheometer plate), the morphology again changes to the isolated disklike aggregates with similar dimensions (~300 nm) as previous ones (Figure 4e). These images indicate that, under the application and release of mechanical stimuli, the small aggregates are dissociated and associated reversibly to demonstrate sol-like and gel-like behaviors. To the best of our knowledge, this is the first report where one can clearly observe the interconversion among different stages of a mechanoresponsive assembly during growth at rest and destruction under shear.

To visualize the influence of temperature, we increased the quenching temperature of **G2** gels periodically, starting from a very low temperature, and studied each stage by SEM (Supporting Information, Figure S12). At very low temperature where the sample behaves like a fluid, the morphology is dominated by the platelike aggregate (the platelike assembly is unable to result in gel formation even after being kept at a constant low temperature for a month). Very interestingly, this morphology changes to one-dimensional aggregates with the increase in temperature to 20 °C and the sample starts to behave like a gel. The above phenomenon scarcely occurs[15] considering the fact that low temperature generally favors gel formation. This means that, in the present case, the substantial

dx.doi.org/10.1021/ja211032m | J. Am. Chem.Soc. 2012, 134, 2161–2171

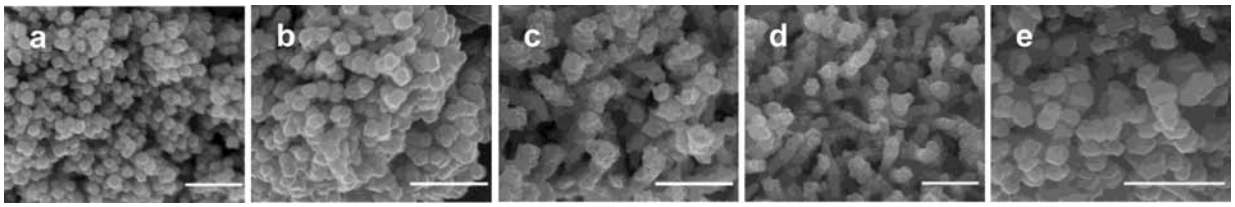

Figure 4. SEM micrographs of **G2** in decalin (1.5% w/v) at 20 °C after different time intervals from mixing with the solvent and homogenizing at 50 °C: (a) 2 h, (b) 5 h, (c) 10 h, (d) 24 h, and (e) after application of shear (scale bar = 1 μm).

thermal motion is a crucial factor that facilitates the one-dimensional aggregate formation. To investigate the effect of higher temperature, we prepared **G2** gels by quenching at 25 and 30 °C. Here again, the morphology changes to the spherical aggregates (at 25 °C), which disappear at 30 °C to build isolated domains, and simultaneously the gel becomes weaker (Supporting Information, Figure S13).

In spite of the fact that **G3** shows only fluidlike behavior, the structural similarity with **G2** prompted us to study the morphology of **G3**. Surprisingly, **G3** forms crystal-like aggregates that have the more or less uniform octagonal shape (~700 nm in dimension) (Figure 5). Very interestingly,

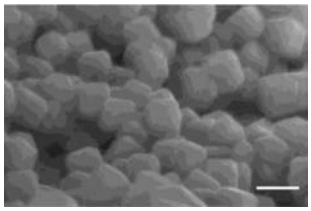

Figure 5. SEM micrograph of **G3** in decalin (1.5% w/v) at 20 °C after 2 weeks of mixing with the solvent and homogenizing at 50 °C (scale bar = 1 μm).

these crystal-like aggregates do not tend to interact among themselves to form any one-dimensional architecture like **G2**, even after several weeks, and still they behave in a fluidlike manner.

In the previous section, we have observed that although **G1** gel is mechanically robust compared to **G2** gel, the former behaves rather ideally and does not show mechanoreponsiveness. Indeed, the morphology of **G1** gel in decalin represents the conventional network structure (Supporting Information, Figure S14) justifying the finding. It is worth noting that the morphological investigation emerges as a helpful tool to monitor and also distinguish among the different types of assemblies, reflecting the different bulk behaviors in terms of gel- or sol-like appearance and responsiveness.

Mechanistic Aspects and Structures of Assemblies. *Preamble to Structural Consideration.* Presently, we have three different kinds of self-assembled systems, namely, **G1**, **G2**, and **G3**, in hand. Among these, **G2** behaves as a thixotropic gel-like material while **G1** acts as a "true gel" and **G3** exhibits a fluidlike appearance. The interesting point is that the constituents of all these systems are the same and consequently the primary interaction sites are similar. It is reasonable to consider, therefore, that the difference in self-assembly behaviors originates solely from two factors: first, the relative orientation of the substituents (hh versus ht) attached to the dianthracene units (in **G2** and **G3**), and second, the structural modification induced by dimerization of the anthracene units. All together, the present systems provide us a unique opportunity to envision how a mechanoresponsive supramolecular assembly grows, differentiating from a conventional thermoresponsive assembly. The thixotropic phenomenon of molecular gels in the literature has been interpreted more commonly via reversible association and dissociation of micro- or nanoscale aggregates, which are spherical,[7e,f] cylindrical,[7g] or fiberlike.[7c,h] In all these cases, the construction of a primary aggregate is indispensable. In the subsequent step, these primary aggregates are capable of building secondary assemblies via weak forces and thus are breakable under shear. However, the driving forces for construction of such primary and secondary assemblies are not specified in detail. Here, to obtain further insights into the aggregation mode, first we shall propose the structures of the different assembled systems based on the primary experimental results and the molecular modeling. Then, using such a model, we shall try to explore the mechanistic detail by which one can reasonably justify other experimental findings. It should also be noted that **G2** and **G3** actually consist of ensembles of stereochemically distinguished molecules. Thus it is hard to propose an absolute molecular model considering all kinds of stereochemistries which differ only minutely from each other. Considering this situation, for simplicity, we shall discuss the structures of the assemblies with the help of *anti*-ht and *syn*-hh stereoisomers for **G2** and **G3**, respectively, as the representatives. We feel that the presence of other stereoisomers (*syn*-ht for **G2** and *anti*-hh for **G3**) would not affect the overall assembly structures, especially for a system that is inherently dynamic in nature. Since the models are not strictly energy-minimized (although close to that), we shall not emphasize the involved energies quantitatively, but we shall discuss the nature of molecular arrangements and the direction of their propagation.

One-Dimensional versus Two-Dimensional Buildup of Assemblies Driven by Intermolecular Interactions. To look into the assembly structure of **G2** and **G3** more closely, we have performed a wide-angle X-ray diffraction study of dried samples obtained from **G2** gel and **G3** (Figure 6a). Since it was very difficult to prepare a good xerogel sample from decalin (due to its high boiling point), this time we used methylcyclohexane for sample preparation, because the overall behaviors of the samples prepared from decalin and methylcyclohexane are very similar, as confirmed from their similar morphologies (Supporting Information, Figure S15) and close gel melting temperatures [T_{gel} values for decalin and methyl cyclohexane gels of **G2** are 45 and 46.5 °C, respectively, for a concentration of 2% (w/v), prepared at 20 °C and measured by the "test tube tilting" method]. Both **G2** and **G3** give similar diffraction patterns consisting of a principal diffraction peak lying in the low-angle region and a diffuse halo lying at a higher angle. While the latter is usually attributed to the disordered alkyl chains,[8c,16] the former sharp diffraction should correspond to a specific repeating distance involved in

dx.doi.org/10.1021/ja211032m | J. Am. Chem.Soc. 2012, 134, 2161−2171

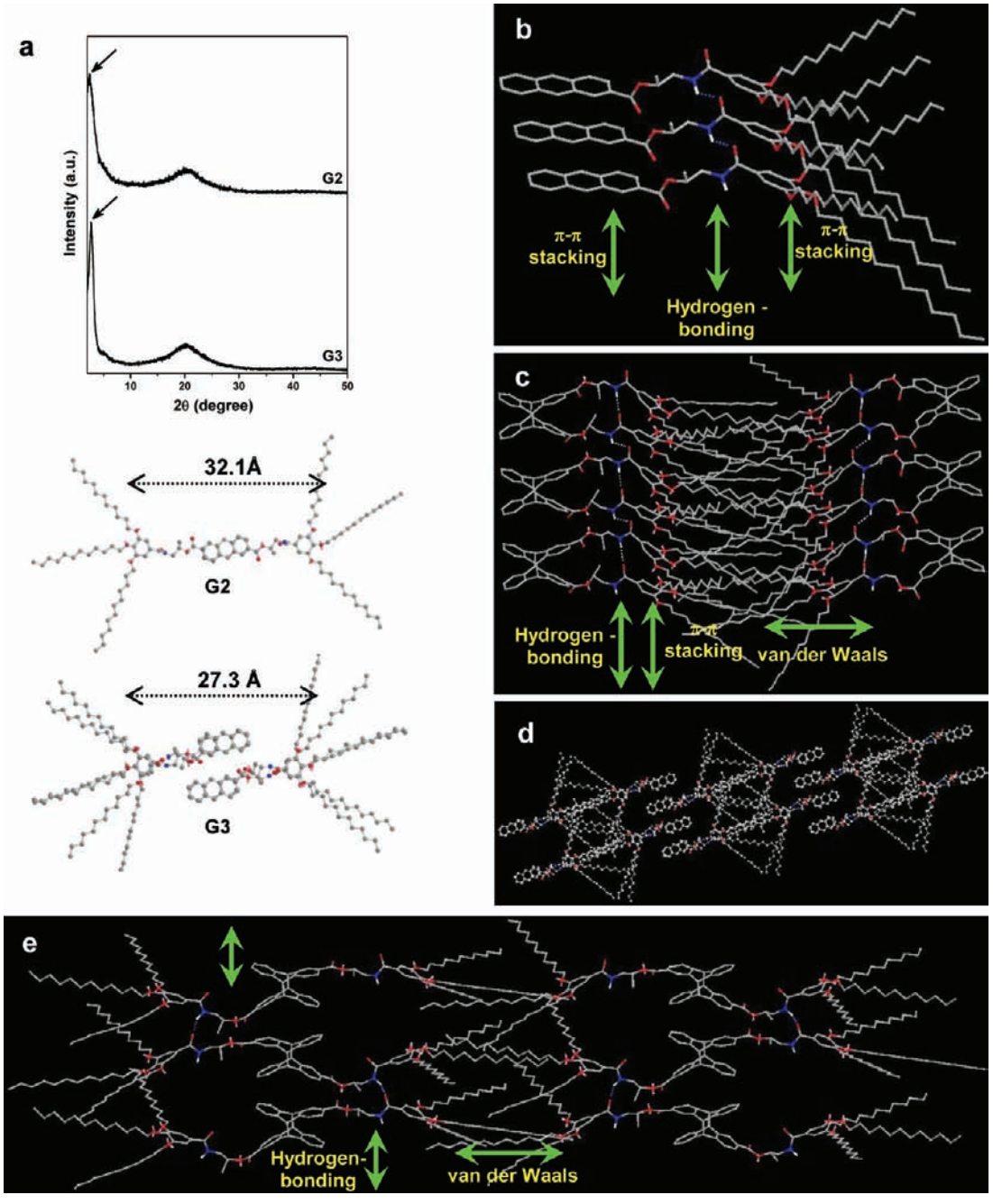

Figure 6. (a) X-ray diffractograms of the dried samples prepared from **G2** gel and **G3** in methylcyclohexane (1.8% w/v) at 20 °C (principal diffraction peaks are indicated with arrows), together with the corresponding molecular spacings assigned for **G2** (for *anti*-ht) and **G3** (for *syn*-hh) with energy-minimized conformations and proposed molecular models for the assemblies of different systems: (b) **G1**, (c) **G3**, (d) top view of further ordering of **G3** (for simplicity only the top layer is shown), and (e) **G2** (green arrows represent the direction of the driving forces for propagation of the assemblies). For simplicity, one type of dimer (*syn*-hh for **G3** and *anti*-ht for **G2**) is considered for model construction.

the assemblies. The differences between **G2** and **G3** diffractions come first in terms of peak positions and second in terms of the associated sharpness. The diffraction peak of **G2** corresponds to a distance of 35.3 Å, which can closely match the molecular length of **G2** (32.1 Å, without consideration of the alkyl chains). On the other hand, the diffraction peak of **G3** corresponds to a distance of 30.4 Å, which is shorter than that of **G2**. Also, the optimized length of a single **G3** molecule is much shorter (16.5 Å) than this distance. To satisfy this spacing, here we have considered a pair of **G3** molecules maintaining the symmetry. This corresponds to an effective distance of 27.3 Å, which closely matches with the diffraction data. Thus it is now reasonable to consider assembly structures where **G2** and **G3** are arranged in an ordered fashion. The sharper appearance of the **G3** diffraction peak probably indicates its higher order of molecular arrangement. On the basis of these primary results, in the next step, we can go into the more detailed structure of **G2** and **G3** assemblies with the help of other experimental results including NMR and morphology, and also by drawing correlations with the monomeric system **G1**, whose assembly structure is fairly straightforward and conventional.

dx.doi.org/10.1021/ja211032m | *J. Am. Chem.Soc.* 2012, 134, 2161−2171

Since the thixotropic gel is a special class of supramolecular gels, we have to realize well how a gel is formed and then we can shed light upon the additional factors that promote the thixotropy. It is well-established that the gelation phenomenon has a close relationship with the process of crystallization. In both cases, growth begins with nucleation. In neat crystallization, molecules gather into two- or three-dimensional objects, whereas in gel formation they grow according to a one-dimensional fashion to construct fibers and eventually form the network structure through entanglement of fibers.[4e,7b,17] Thus, the prerequisite factors for gelation are first, the presence of strong and directional intermolecular interactions; second, the ability to form intertwined aggregates by comparatively weaker interactions; and third, the presence of factors to inhibit neat crystallization. Existence of strong intermolecular hydrogen-bonding sites is commonly favorable to impose the first factor, whereas the presence of long alkyl chains fulfills other two factors.

Keeping the above-mentioned points in our mind, we previously designed gelator **G1**, which was capable of gelating organic solvents. **G1** possesses two primary interaction sites: the amide linkage, capable of forming intermolecular hydrogen bonding, and the anthracene moiety and the benzene ring (in gallic acid), for $\pi-\pi$ stacking interactions. From HPLC analysis of dimerized **G1**, it is clearly revealed that **G1** selectively orients in a hh manner in the decalin gel (Supporting Information, Table S2). Also, the formation of intermolecular hydrogen bonding and J-type aggregates is evident from NMR and the red shift of absorption and emission maxima upon gelation (Supporting Information, Figure S16). Simply on the basis of these experimental results, we can propose a molecular model for **G1** assembly (Figure 6b).[18] It appears from the modeling study that the driving forces for propagation of the assembly into one dimension are very strong because of the cooperative contributions from intermolecular hydrogen bonding and $\pi-\pi$ stacking interactions. Altogether this is a three-point interaction, all of which facilitates the assembly to grow in one direction. Undoubtedly, such a scenario satisfies the prerequisite criteria for gelation and therefore the sample exhibits a fibrous morphology (Supporting Information, Figure S14) and acts as a "true" gel in terms of rheological behavior (Supporting Information, Figure S8). Here, the presence of van der Waals type interaction (rather weak compared to the strong $\pi-\pi$ stacking and intermolecular hydrogen-bonding interaction) arising from the long alkyl chains would only facilitate the interfibrillar interaction to build a network structure.

Upon dimerization, $\pi-\pi$ stacking interaction between two anthracene units is eliminated due to the formation of covalent bonds (cycloaddition). It seems unreasonable to consider the stacking interaction among the dianthracenes (having separated benzene rings) because of their bent structure. Hence, the possible stacking interaction may arise only from the gallic acid moieties, which again is not strong owing to the presence of the single benzene ring. For **G2** and **G3**, therefore, the intermolecular hydrogen-bonding interaction is expected to play the key role in the assembly process. The formation of hydrogen bonds in **G2** and **G3** in decalin is evident from NMR (Supporting Information, Figure S17).[19] The significant broadening of the NMR signals assigned to dianthracene protons indicates some sort of interaction among them. The striking difference in the NMR spectra of **G2** and **G3** in decalin-d_{18} is observed for the signals of the aromatic protons in gallic acid. The signal at 6.78 ppm corresponds to unstacked (or free) gallic acid protons, whereas the signals between 6.55 and 6.74 ppm correspond to stacked gallic acid protons. Only **G2** executes a strong signal at 6.78 ppm. The corresponding signal of **G3** is very weak; instead, it gives broad and intense signals between 6.55 and 6.74 ppm. This means that in **G3** (though it is fluidlike) the molecular motion of gallic acid moieties is substantially restricted, which signifies a fair amount of interaction among them. These results prompted us to propose the models for **G3** and **G2** as depicted in Figure 6c and 6e, respectively. In the case of **G3**, the assembled structure can involve intra- as well as intermolecular hydrogen bonding (Figure 6c).[20] However, the absence of efficient $\pi-\pi$ stacking among the dianthracenes would allow us to consider that intermolecular hydrogen bonding should be weaker and also less favored compared to intramolecular hydrogen bonding. On the other hand, strong van der Waals interaction is probable in the orthogonal direction via the alkyl chains oriented on the same side of dianthracene. Thus, the driving forces for propagation of assembly in two dimensions are comparable. This situation differs significantly from that of **G1**, where the driving force for propagation in one direction (via cooperative contributions from $\pi-\pi$ stacking and intermolecular hydrogen-bonding interaction) was predominant compared to that in the other direction (via much weaker van der Waals interaction). According to earlier reports,[21] the presence of long alkyl chains facilitates gelation, whereas the presence of short alkyl chains or branching favors solubilization or crystallization. The hh orientation, in which the alkyl chains are oriented in the same direction, is closer to the second scenario. As a result, we could obtain a crystalline aggregate of definite shape (nearly octagonal block) having a dimension of ~700 nm (Figure 5). The presence of a very sharp diffraction peak in the XRD diffractogram also supports the highly ordered assembly structure of **G3**. It is interesting to note that these crystalline aggregates do not interact further (even after several weeks) to build any secondary assembly and remain fluidlike. Considering the spacing assigned in Figure 6a and primary assembly depicted in Figure 6c, we can propose another model for subsequent ordering of **G3** molecules (Figure 6d), which may lead to the formation of crystalline aggregates of definite shape.

Finally, in the case of **G2**, the intermolecular hydrogen bonding (intramolecular hydrogen bonding is not possible here) is rather weak in the absence of the $\pi-\pi$ stacking interactions among the dianthracenes or among the gallic acid moieties (Supporting Information, Figure S17). Here, the assembly tends to propagate in two dimensions with weak driving forces (Figure 6e). We can thus consider the present system as the intermediate between **G1** and **G3**. In one way, the lack of predominant unidirectional propagation does not result in a true fibrous gel, and at the same time, the lack of compactness and orderliness arising from the van der Waals interaction (weaker than **G3**) composed of long akyl chains oriented in opposite directions, inhibit the formation of regular crystalline aggregate. As evident from the XRD data (Figure 6a), however, the intermolecular interactions are enough to result in the formation of a fairly ordered (less than that of **G3**) primary assembly. Thus, at the initial stage, discrete disklike aggregates of irregular shapes (Figure 4a) with smaller dimensions (~ 300 nm) are seen. In subsequent steps, this primary assembly can build a secondary assembly (preferably via van der Waals interaction) (Figure 4d), which is actually a pseudo-one-dimensional arrangement, and ultimately we obtained a thixotropic gel. Here, the specialty is the finding

that the pseudo-one-dimensional arrangement can be broken easily by shear to regenerate the primary assemblies (Figure 4e), and this process is reversible.

Factors Favoring Thixotropy. The essence of the above observations and interpretations is summarized in Scheme 2,

Scheme 2. Cartoon Presentation of Self-Assembly Process of G2 with Time and under Shear[a]

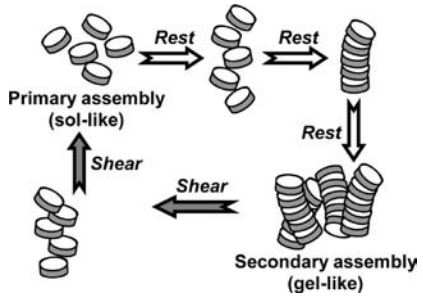

[a]For simplicity, the irregular-shaped primary assemblies are approximated as "disklike".

where one can image the reversible interconversion between primary and the secondary assemblies under mechanical stimuli. This illustration corresponds perfectly to the SEM observations as depicted in Figure 4. Probably, the destruction of the secondary assembly is a sequential process, which is reflected by the two-step breaking in the rheological experiment (Supporting Information, Figure S4). From the present study, it appears that, to qualify as a thixotropic gel, a few criteria are essential for the LMGs: (i) the presence of long-range weak interaction and (ii) capacity to propagate in more than one dimension or, in other words, possessing comparable driving forces for propagating in either direction. The LMG with low crystallinity should facilitate the above situation. **G1** gel possessing the fibrous morphology, on the other hand, undergoes disassembly of the network and irreversible cleavage of the fibers under shear (Supporting Information, Scheme S1). Therefore, the fragmented fibers (which resemble with the primary assembly in thixotropic gels) are indefinite and irregular and thus they cannot rebuild the network unless they are heated to the homogenized phase again. In other words, the presence of definite junction zones is indispensable for reversible transition between primary and secondary assemblies. Also, due to the presence of strong intermolecular interaction, **G1** gel is more resistant against the applied stress, as evident from the higher storage modulus and yield stress values than those of **G2**.

Temperature plays an important role in the growth of **G2** assembly, as we observed from the morphological study. Low quenching temperatures give only two-dimensional aggregates that fail to immobilize the solvent. However, once we put the same sample at room temperature (~20 °C), it forms a gel. This means that, at room temperature, the presence of thermal fluctuation actually facilitates the primary assemblies to interact, forming the secondary assembly that ultimately promotes the gelation. With further increase in temperature, the gel becomes weaker due to destabilization of the secondary assembly (at 25 °C) or even the primary assembly (at 30 °C). Probably, the presence of relatively weak interactions in **G2** assembly induces such sensitivity toward the thermal history. Thus, the shape and stereochemistry of the dimeric gelators differentiate them from the monomeric one by modifying the intermolecular interactions, and as a result we could obtain a variety of supramolecular assemblies executing different responsiveness.

The above discussion has clearly explained, for the first time, the relationship between gelator structure and mechanoresponsiveness, which is essential for the future study and design of such "dynamic" assembly systems.

Mechanoresponsive Assembly in the Presence of Fullerenes. *Fullerenes as Guest.* In the process of utilizing our mechanoresponsive supramolecular assemblies for hosting suitable functional guests, the first priority was to retain the thixotropic behavior of the host. Presence of soft interaction between host and guest would facilitate such a situation. In other words, the added guest should not interrupt the primary interactions among **G2**, however, complexation and decomplexation can still occur reversibly under the stimuli. In this regard, we considered fullerenes as a most suitable class of guest molecules for three reasons: first, the concave shape of dianthracene moiety is expected to enjoy efficient van der Waals contact with the convex surface of fullerenes; second, since the van der Waals interaction would be the principal driving force behind such a binding, it might be possible to disintegrate the complex under shear; and finally, fullerene might act like a molecular adhesive to create junction points that would facilitate thixotropic behavior.

In our study, we used two types of fullerene, C_{60} and C_{70}. The former has a spherical shape whereas the latter can be considered as a diffuse sphere. First, we prepared saturated solutions of fullerenes in decalin at 20 °C (diluted when necessary) and then mixed them with **G2** in a similar fashion as we did without fullerenes. Very interestingly, the mixed systems form gels that indeed exhibit thixotropy (Supporting Information, Figure S18). As expected, these gels are also thermoreversible. It should be noted that, even in the presence of fullerenes, **G2** forms the gel only near room temperature. This signifies that probably the binding of fullerene does not alter the basic supramolecular aggregation mode of **G2**. Therefore, one of our prerequisite criteria is fulfilled.

Influence of Fullerenes on G2 Assembly. The next important issue to address is the rheological behavior of **G2** in the presence of fullerenes. The dynamic frequency sweep experiment shows similar frequency dependency of the elastic and viscous moduli (Supporting Information, Figure S19), signifying structural relaxation. This means that even in the presence of fullerenes, **G2** assembly retains its dynamic character. Actually, the dynamic character increases in the order **G2** < **G2**-C_{60} < **G2**-C_{70} as evident from the shift of the crossover point between G' and G'' toward higher frequencies. The superior elastic behavior of **G2**-C_{60} and **G2**-C_{70} gels is well reflected in their storage moduli and also in yield stress values, which increase in the order **G2** < **G2**-C_{60} < **G2**-C_{70} (Supporting Information, Figure S20). Finally, the thixotropic behavior of the samples was tested by time evolution of the storage modulus after the gels were destroyed by shear. It is worth noting that thixotropic behavior is also enhanced in the order **G2** < **G2**-C_{60} < **G2**-C_{70} in terms of faster recovery of the storage modulus (Figure 7). Thus, the presence of fullerenes not only improves the mechanical property of **G2** assembly but also intensifies its thixotropic behavior. As expected, the morphologies of **G2**-C_{60} and **G2**-C_{70} gels are somewhat modified, however, the compound nature of the secondary assemblies remains similar to that of **G2** (Figure 8).

Binding of Fullerenes to G2. Since dianthracene is not an efficient donor, van der Waals interaction is expected to take

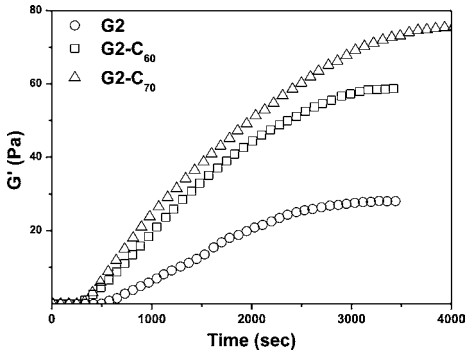

Figure 7. Evolution of storage modulus G' as a function of time for **G2**, **G2**-C_{60}, and **G2**-C_{70} assemblies in decalin (1.8% w/v) performed at 20 °C under 1% strain and at a frequency 100 rad/s (**G2**:fullerenes = 8:1 mol/mol).

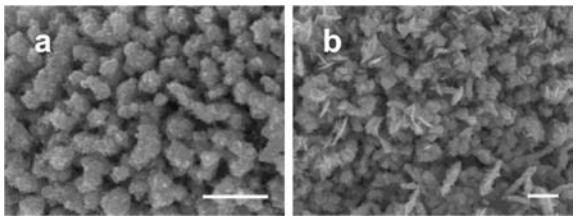

Figure 8. SEM micrographs of (a) **G2**-C_{60} and (b) **G2**-C_{70} gels in decalin (1.5% w/v) at 20 °C prepared by homogenization at 50 °C (scale bar = 1 μm) (**G2**:fullerenes = 8:1 mol/mol).

the leading role in complex formation. That is why we have not found any signature charge-transfer band in UV–vis spectra of **G2**-C_{60} solution in decalin. Since the UV–vis spectrum was not so informative, we tried to determine the association constant involved in binding of fullerenes with **G2** qualitatively by using a solvent extraction method, which is a classical approach for investigating metal–ligand binding.[22] Here, we used hexane, which is a poor solvent of fullerenes, for the extraction (details of the method and working equation are given in the Supporting Information).[23] It is interesting to note that the association constant of C_{70} with **G2** is 2 times higher than that of C_{60} (Supporting Information, Tables S3 and S4). This means that **G2** has greater affinity for C_{70} compared to C_{60}. However, since their binding constants are in the same range, **G2** does not exhibit a high degree of selectivity. Another important issue is determination of the binding site of fullerenes with **G2**. There are two probable binding sites available in **G2**: the dianthracene moiety and the benzene ring in the gallic acid moiety. From NMR spectroscopy, we can clearly observe a change in the signals corresponding to a group of dianthracene aromatic protons upon addition of fullerenes (Supporting Information, Figure S21). On the other hand, in the presence of C_{60} and C_{70}, aromatic protons in gallic acid remain practically unaltered. This is evidence that the fullerenes preferably bind to the dianthracene moiety in **G2**. This is also consistent with previous reports where the concave hosts favor the fullerene binding arising from the concave–convex complementarity.[9]

*Proposed Structures of **G2**–Fullerene Assemblies.* From the above results, it is evident that the basic structure of **G2** assembly remains practically unaltered even in the presence of fullerenes, including the formation of intermolecular hydrogen bonding (Supporting Information, Figure S22). Keeping the above points in mind, we have proposed molecular models for **G2**-C_{60} and **G2**-C_{70} assemblies (Supporting Information, Figure S23), where each fullerene molecule is sandwiched between two dianthracene units without affecting the overall assembly. Incorporation of fullerene is expected to increase the spacing between two dianthracene units, thereby inhibiting the interaction among themselves, which is reflected in the NMR spectra (Supporting Information, Figure S21). The fullerenes act like "junction zones" in the **G2** assembly, facilitating shear-induced destruction and also faster recovery upon resting. This situation is opposite to a recent report where an added guest molecule inhibits the existing gel structure due to the formation of capsulelike assembly via the strong host–guest interaction.[24] This justifies the indispensability of the soft-mode interaction between host and guest in our study. Superiority of C_{70} in binding with **G2** and also in executing thixotropy probably originates from its better fit with the concave dianthracenes.

In summary, the presence of fullerenes adds two important contributions to the mechanoresponsive assembly of **G2**: first, the elastic property of the assembly is enhanced, and second, mechanoresponsiveness is also intensified. To the best of our knowledge, this is the first report of mechanoresponsive assembly of fullerenes.

CONCLUSIONS

In conclusion, comparative supramolecular assemblies of a substituted anthracene-based gelator **G1** and its corresponding dimers **G2** and **G3** have been investigated. Cooperative contributions from intermolecular hydrogen bonding and π–π stacking interactions facilitate the formation of one-dimensional molecular arrangement of **G1** and it gives an ideal gel in decalin, exhibiting frequency-independent storage and loss modulus in a frequency sweep experiment. Upon dimerization, **G1** produces hh- and ht-type dimers where the π–π stacking interaction among the dianthracene units has been eliminated, first due to the cycloaddition process and second because of the structural modification from planar anthracene to concave dianthracene moiety. Then, the next factor, that is, relative orientation of the substituent, consequently emerges. **G3**, which is dominated by hh-type orientation, behaves as fluidlike. Most interesting is the behavior of **G2**, which is dominated by ht-type dimer orientation. It forms a mechanoresponsive gel-like material as well as demonstrating the signature of a structural relaxation process as evident from its frequency-dependent elastic and viscous moduli. In the growth of **G2** assembly, two-dimensional propagation leads to the formation of primary assembly, composed of disklike nanoaggregates, which in the next step interact to construct the densely packed secondary assembly and exhibit gel-like behavior. The phenomenon of mechanoresponsiveness originates from the reversible transition between the primary and secondary assemblies under shear and upon resting. On the other hand, **G3** forms crystal-like aggregates in the primary assembly process and these nanocrystals cannot form any secondary assembly, and the system behaves as fluidlike. Presence of long-range weak interactions and the driving forces capable of propagating in more than one dimension thus emerged as the principal factors behind the construction of such a mechanoresponsive assembly. Addition of fullerenes acting as soft junction points enhances the mechanical properties and responsiveness of **G2** assembly remarkably. Due to the better fit with the concave host, C_{70} emerges as a superior additive over C_{60} in terms of improving mechanical properties and thixotropy.

dx.doi.org/10.1021/ja211032m | J. Am. Chem.Soc. 2012, 134, 2161–2171

Therefore, the significance of the present work is three-fold: first, we have succeeded in developing a mechanoresponsive supramolecular assembly where the assembly phenomenon is governed by the orientation of the substituents; second, we could apply this system to act as the host for functional materials like fullerenes to develop mechanoresponsive fullerene assemblies for the first time; and finally, we have made a genuine attempt to correlate as well as differentiate between mechanoresponsive and thermoresponsive assemblies, simultaneously highlighting the underlying factors favoring growth of a mechanoresponsive supramolecular assembly. We believe, therefore, that the current work would offer a firm mechanistic background for the design of thixotropic materials, by eliminating the "serendipity" expected so far in developing such materials.[25]

EXPERIMENTAL SECTION

Synthesis of G1, G2, and G3. **G1** was synthesized according to the method described earlier.[8c] **G2** and **G3** were synthesized by photodimerization of **G1** in tetrahydrofuran (THF) at 40 °C and in methylcyclohexane at 30 °C, respectively (Supporting Information, Table S1). After the photoreaction, the solvents were evaporated at room temperature and the photodimers were used without further purification. Matrix-assisted laser desorption ionization time-of-flight mass spectroscopy (MALDI-TOF MS) (dithranol): m/z calcd for [M + Na], 1895.39; found, 1896.17 and 1895.69 for **G2** and **G3**, respectively. The structures of **G2** and **G3** were evaluated by HPLC analysis (see Supporting Information).[8a,26] Dimerization was confirmed by NMR and UV−vis spectroscopy (Supporting Information, Figures S1 and S2).

ASSOCIATED CONTENT

Supporting Information

Additional text, 23 figures, four tables, and one scheme, showing experimental details, HPLC analysis results, spectroscopic and rheological data, SEM observations, detailed procedure for determination of association constants, and molecular models. This material is available free of charge via the Internet at http://pubs.acs.org.

AUTHOR INFORMATION

Corresponding Author

shinkai_center@mail.cstm.kyushu-u.ac.jp

ACKNOWLEDGMENTS

Financial support was provided by MEXT by a Grant-in-Aid for Scientific Research on Innovative Areas "Emergence in Chemistry" (20111011). We thank Dr. S.-i. Tamaru of Sojo University for NMR measurements.

REFERENCES

(1) (a) Lehn, J.-M. *Supramolecular Chemistry*; VCH: Weinheim, Germany, 1995. (b) Steed, J. W.; Atwood, J. L. *Supramolecular Chemistry*, 2nd ed.; J. Wiley & Sons: Chichester, U.K., 2009.

(2) (a) Terech, P.; Weiss, R. G. *Chem. Rev.* **1997**, *97*, 3133. (b) Abdallah, D. J.; Weiss, R. G. *Adv. Mater.* **2000**, *12*, 1237. (c) Gronwald, O.; Snip, E.; Shinkai, S. *Curr. Opin. Colloid Interface Sci.* **2002**, *7*, 148. (d) van Bommel, K. J. C.; Friggeri, A; Shinkai, S. *Angew. Chem.* **2003**, *115*, 1010; *Angew. Chem., Int. Ed.* **2003**, *42*, 980. (e) Ajayaghosh, A.; Praveen, V. K.; Vijayakumar, C. *Chem. Soc. Rev.* **2008**, *37*, 109. (f) Banerjee, S.; Das, R. K.; Maitra, U. *J. Mater. Chem.* **2009**, *19*, 6649. (g) Smith, D. K. *Chem. Soc. Rev.* **2009**, *38*, 684. (h) Dawn, A; Shiraki, T.; Haraguchi, S.; Tamaru, S-i.; Shinkai, S. *Chem.—Asian. J.* **2011**, *6*, 266.

(3) (a) Sangeetha, N. M.; Maitra, U. *Chem. Soc. Rev.* **2005**, *34*, 821. (b) Maeda, H. *Chem.—Eur. J.* **2008**, *14*, 11274. (c) Piepenbrock, M.-O. M.; Lloyd, G. O.; Clarke, N.; Steed, J. W. *Chem. Rev.* **2010**, *110*, 1960.

(4) (a) van Esch, J. H.; Feringa, B. L. *Angew. Chem.* **2000**, *112*, 2351; *Angew. Chem., Int. Ed.* **2000**, *39*, 2263. (b) Pozzo, J.-L.; Clavier, G. M.; Desvergne, J.-P. *J. Mater. Chem.* **1998**, *8*, 2575. (c) Tamaru, S-i.; Nakamura, M.; Takeuchi, M.; Shinkai, S. *Org. Lett.* **2001**, *3*, 3631. (d) Mieden-Gundert, G.; Klein, L.; Fischer, M.; Vogtle, F.; Heuze, K.; Pozzo, J.-L.; Vallier, M.; Fages, F. *Angew. Chem.* **2001**, *113*, 3266; *Angew. Chem., Int. Ed.* **2001**, *40*, 3164. (e) Dastidar, P. *Chem. Soc. Rev.* **2008**, *37*, 2699.

(5) (a) Beyer, M. K.; Clausen-Schaumann, H. *Chem. Rev.* **2005**, *105*, 2921. (b) Hickenboth, C. R.; Moore, J. S.; White, S. R.; Sottos, N. R.; Baudry, J.; Wilson, S. R. *Nature* **2007**, *446*, 423. (c) Davis, D. A.; Hamilton, A.; Yang, J.; Cremar, L. D.; Gough, D. V.; Potisek, S. L.; Ong, M. T.; Braun, P. V.; Martınez, T. J.; White, S. R.; Moore, J. S.; Sottos, N. R. *Nature* **2009**, *459*, 68.

(6) Carrion-Vazquez, M.; Oberhauser, A. F.; Fisher, T. E.; Marszalek, P. E.; Li, H.; Fernandez, J. M. *Prog. Biophys. Mol. Biol.* **2000**, *74*, 63.

(7) (a) van Esch, J.; Schoonbeek, F.; de Loos, M.; Kooijman, H.; Spek, A. L.; Kellogg, R. M.; Feringa, B. L. *Chem.—Eur. J.* **1999**, *5*, 937. (b) Brinksma, J.; Feringa, B. L.; Kellogg, R. M.; Vreeker, R.; van Esch, J. *Langmuir* **2000**, *16*, 9249. (c) Lescanne, M.; Grondin, P.; d'Aleo, A.; Fages, F.; Pozzo, J.-L.; Monval, O. M.; Reinheimer, P.; Colin, A. *Langmuir* **2004**, *20*, 3032. (d) Shirakawa, M.; Fujita, N.; Shinkai, S. *J. Am. Chem. Soc.* **2005**, *127*, 4164. (e) Huang, X.; Raghavan, S. R.; Terech, P.; Weiss, R. G. *J. Am. Chem. Soc.* **2006**, *128*, 15341. (f) Liu, J.; He, P.; Yan, J.; Fang, X.; Peng, J.; Liu, K.; Fang, Y. *Adv. Mater.* **2008**, *20*, 2508. (g) Percec, V.; Peterca, M.; Yurchenko, M. E.; Rudick, J. G.; Heiney, P. A. *Chem.—Eur. J.* **2008**, *14*, 909. (h) Mukhopadhyay, P.; Fujita, N.; Takada, A.; Kishida, T.; Shirakawa, M.; Shinkai, S. *Angew. Chem.* **2010**, *122*, 6482; *Angew. Chem., Int. Ed.* **2010**, *49*, 6338.

(8) (a) Dawn, A.; Fujita, N.; Haraguchi, S.; Sada, K.; Shinkai, S. *Chem. Commun.* **2009**, 2100. (b) Dawn, A.; Fujita, N.; Haraguchi, S.; Sada, K.; Tamaru, S-i.; Shinkai, S. *Org. Biomol. Chem.* **2009**, *7*, 4378. (c) Dawn, A.; Shiraki, T.; Haraguchi, S.; Sato, H.; Sada, K.; Shinkai, S. *Chem.—Eur. J.* **2010**, *16*, 3676.

(9) (a) Konarev, D. V.; Valeev, E. F.; Slovokhotov, Y. L.; Shul'ga, Y. M.; Lyubovskaya, R. N. *J. Chem. Res. (S)* **1997**, 442. (b) Mizyed, S.; Georghiou, P.; Bancu, M.; Cuadra, B.; Rai, A. K.; Cheng, P.; Scott, L. T. *J. Am. Chem. Soc.* **2001**, *123*, 12770. (c) Georghiou, P.; Tran, A. H.; Mizyed, S.; Bancu, M.; Scott, L. T. *J. Org. Chem.* **2005**, *70*, 6158. (d) Perez, E. M.; Martın, N. *Chem. Soc. Rev.* **2008**, *37*, 1512.

(10) (a) Ward, S. M. V.; Weins, A.; Pollak, M. R.; Weitz, D. A. *Biophys. J.* **2008**, *95*, 4915. (b) Hoffmann, I.; Heunemann, P.; Prevost, S.; Schweins, R.; Wagner, N. J.; Gradzielski, M. *Langmuir* **2011**, *27*, 4386.

(11) Dreiss, C. A. *Soft Matter* **2007**, *3*, 956 and references therein.

(12) Lescanne, M.; Colin, A.; Mondain-Monval, O.; Fages, F.; Pozzo, J.-L. *Langmuir* **2003**, *19*, 2013.

(13) To test the influence of unconverted **G1** (if there is any), we have performed the same experiment with **G1**/**G2** mixture (50% by weight) in decalin (Supporting Information, Figure S6). It is observed that, compared to **G2**, the value of G' is negligibly small for **G1**/**G2** mixture and no detectable changes can be observed upon application and release of shear. Thus, the presence of **G1** does not contribute either to the gel formation or to the mechanoresponsiveness.

(14) Weng, W.; Beck, J. B.; Jamieson, A. M.; Rowan, S. J. *J. Am. Chem. Soc.* **2006**, *128*, 11663.

(15) (a) Kuroiwa, K.; Shibata, T.; Takada, A.; Nemoto, N.; Kimizuka, N. *J. Am. Chem. Soc.* **2004**, *126*, 2016. (b) Paulusse, J. M. J.; van Beek, D. J. M.; Sijbesma, R. P. *J. Am. Chem. Soc.* **2007**, *129*, 2392.

(16) Wurthner, F.; Thalacker, C.; Diele, S.; Tschierske, C. *Chem.—Eur. J.* **2001**, *7*, 2245.

(17) (a) Hanabusa, K.; Yamada, M.; Kimura, M.; Shirai, H. *Angew. Chem., Int. Ed. Engl.* **1996**, *35*, 1949. (b) Luboradzki, R.; Gronwald, O.;

Ikeda, M.; Shinkai, S.; Reinhoudt, D. N. *Tetrahedron* **2000**, *56*, 9595. (c) George, M; Weiss, R. G. *Acc. Chem. Res.* **2006**, *39*, 489.
(18) The XRD pattern of the xerogel of **G1** prepared from methylcyclohexane can be found in ref 8c.
(19) The signal corresponding to the amide proton located at 50 °C disappeared at 20 °C and probably shifted downfield and merged with the other signals.
(20) The concentration-dependent NMR spectra of the sample were not enough to distinguish between two types of hydrogen bonding due to broadening of the signals.
(21) (a) Shirakawa, M.; Kawano, S.-i.; Fujita, N.; Sada, K.; Shinaki, S. *J. Org. Chem.* **2003**, *68*, 5037. (b) Shirakawa, M.; Fujita, N.; Tani, T.; Kaneko, K.; Shinkai, S. *Chem. Commun.* **2005**, 4149. (c) Mukhopadhyay., P.; Iwashita, Y.; Shirakawa, M.; Kawano, S-i; Fujita, N.; Shinkai, S. *Angew. Chem., Int. Ed.* **2006**, *45*, 1592.
(22) (a) Hongwu, Y; Zhixian, Z.; Mingrui, Z.; Xianxin, Z.; Boyang, R. *Polyhedron* **1991**, *10*, 1025. (b) Kolthoff, I. M.; Chantooni, M. K. Jr. *J. Chem. Eng. Data* **1993**, *38*, 556. (c) Wacker, P.; Kleinpeter, E. *J. Inclusion Phenom. Macrocyclic Chem.* **2007**, *59*, 331.
(23) We were unable to determine the stoichiometry of the complex precisely because the host–guest interaction is rather weak and also we were dealing with the mixture of gelators. As an approximation, we used 1:1 binding for calculation of the association constants.
(24) Tiefenbacher, K.; Dube, H.; Ajami, D; Rebek, J. *Chem. Commun.* **2011**, *47*, 7341.
(25) One reviewer suggested that the reversible photoconversion between monomeric and dimeric systems could be useful to apply our systems for imaging or information storage. However, first, we have noticed that dimer to monomer conversion under UV irradiation is rather inefficient in our system, because the absorption maximum of dianthracene overlaps with that of the gallic acid moiety. Second, the dimeric gelator **G2** is dominated by ht-type dimers; however, ht-type orientation does not favor gel formation in the case of monomeric gelator **G1**. At the same time **G1** gel is dominated by hh-type orientation, which upon dimerization would result in the formation of **G3** (not **G2**). Thus, direct photoreversible conversion between **G1** gel and **G2** gel is also not possible here.
(26) Nakamura, A.; Inoue, Y. *J. Am. Chem. Soc.* **2003**, *125*, 966.